Hindawi
Mobile Information Systems
Volume 2022, Article ID 1478626, 10 pages
https://doi.org/10.1155/2022/1478626

Research Article

Sports Personnel Health Monitoring Application Based on Biometric Data Collection Model

Xueqing Hu

Sports Department, Jiangsu University, Zhenjiang, Jiangsu 212013, China

Correspondence should be addressed to Xueqing Hu; 2020020194@stu.cdut.edu.cn

Received 25 May 2022; Revised 11 July 2022; Accepted 16 July 2022; Published 8 August 2022

Academic Editor: Chi Lin

In order to improve the health monitoring effect of sports personnel, this study combines the biometric data acquisition model to construct the sports personnel health monitoring application program. Moreover, this study uses the iterative conjugate gradient method ICGM to prove the correctness of the biometric data acquisition algorithm from the changes of the residual and the objective function in the iterative process. Finally, the optimized cosine similarity is substituted into the SBGI model, and better results are obtained than using the weighted cosine similarity as input. The research shows that the sports personnel health monitoring application based on the biometric data collection model proposed in this study has a good health monitoring effect, and has an important supporting role in improving the fitness effect of group sports.

1. Introduction

The acquisition and transmission of fitness exercise data mainly include two aspects: exercise effect and exercise equipment data. Heart rate data are an important indicator to reflect the exercise effect of practitioners, especially aerobic exercise [1]. Moreover, the size of the heart rate and the speed at which the heart rate returns to normal reflect the physical condition of the practitioner and the effect of the exercise. At the same time, the heart rate data should be matched with specific exercise equipment for analysis. The heart rate changes in aerobic training and the heart rate changes in resistance training are different, and need to be fully excavated [2]. In this study, the heart rate sensor was used to obtain the heart rate data of the exerciser, and the information of the exercise equipment was obtained through the radio frequency identification technology [3].

Fitness exercise can effectively improve physical health, but exercise with a too low heart rate will not have a good training effect, and exercise with a high heart rate increases the risk of training. The basic information of the practitioner, such as name, gender, age, height, and weight, can be read through the smart device, and the maximum heart rate can be calculated based on age and resting heart rate. According to the impact of different heart rate zones on exercise, heart rate zones can be divided into four stages. Among them, the heart rate zone in the warm-up phase is 50%–60% of the maximum heart rate. At this stage, the exercise intensity is relatively low, and it is generally a preparatory activity to improve the function of the body and prevent injury. The heart rate zone during the fat-burning phase is 60%–70% of the maximum heart rate. The intensity of exercise at this stage is greater than that of the warm-up stage. As long as the amount of exercise is reasonable, it will have a good effect of burning fat. Therefore, this stage is of great help to those who need to lose fat. In the endurance phase, the heart rate zone is 70%–80% of the maximum heart rate. At this stage, the exercise intensity is higher than that of the fat-burning stage, and the durability of exercise is lower, but it is of great help to improve the cardiovascular system and respiratory system. Therefore, this stage is more suitable for people who need to improve their cardiopulmonary function. The heart rate in the strength training phase should be above 80% of the maximum heart rate. In this phase, the exercise intensity is very high, the muscle burden is relatively large, and it is easy to cause fatigue. Therefore, this stage is very helpful for muscle growth and is suitable for people who need to improve muscle strength and endurance. Through Internet

technology, the heart rate data of the user during exercise are obtained. Then, according to the needs of users, the system analysis is carried out. For users who need to lose fat, the recommended heart rate range is 60%–80% of the maximum heart rate (fat-burning exercise and aerobic endurance stage), and for users who need to build muscle, it is recommended that the heart rate be more than 80% of the maximum heart rate (strength exercise stage). In addition, monitoring the heart rate of fitness exercise can improve exercise effect, reduce exercise risk, and make fitness exercise more scientific and professional.

In this study, a biometric data collection model is combined to construct a sports personnel health monitoring application program to improve the health monitoring effect of sports personnel.

2. Related Work

Literature [4] designed a telemedicine monitoring system based on ZigBee sensor and wireless local area network, which can realize remote medical monitoring of sick patients at home; Literature [5] proposed to popularize healthy life, build a healthy environment, improve health protection, optimize health services, and develop health industries to comprehensively promote the construction of a healthy China and achieve the grand goal of a healthy China. Literature [6] designed a new type of human health monitoring system based on ZigBee and IGPS positioning technology. The system combines ZigBee technology and smartphones. It not only has the characteristics of low cost, low power consumption, reliable data transmission, and strong anti-interference ability, which reduces the hardware cost, but also improves the system stability and portability, and meets the needs of human health monitoring requirements. As far as the current policies and markets are concerned, its development prospects are very broad.

Literature [7] studies and designs a human vital index detection terminal with a shape similar to a ring. This terminal can realize the collection of human blood oxygen saturation, heart rate information, and pulse information; a French company designed a human health data collection The gloves can realize the collection of human health data such as human skin blood flow velocity, skin conductivity, instantaneous heart rate, and respiration. The system can realize the analysis and processing of health data to obtain the state of human health; Literature [8] developed a portable terminal for the collection and monitoring of human physiological data can collect ECG, blood pressure, body temperature data, and at the same time can realize fall detection and alarm; Literature [9] developed a system for children's health monitoring based on mobile phones; Literature [10] proposed A system equipped with a heart rate sensor to collect the patient's heart rate data, and send the data to the Web terminal remotely via wireless means for doctors and nurses to view. Smart medical care and mobile medical care have attracted the attention of some other mobile medical and medical equipment providers, and they have carried out research in the field of smart medical care. A product designed by MobileOCT, which uses mobile phones, cameras, and algorithms to detect sports health [11]; the system designed in Literature [12] can collect body temperature, ECG, and blood oxygen data, and send the collected data through Bluetooth. Give users a mobile phone for users to view; an APP designed in the literature [13] can realize the functions of collecting sensor data and data analysis, through which it can improve the user's mental health status, and can be applied to depression, chronic pain, and other ailments. In nursing and treatment, improve the effect of treatment and nursing; Literature [14] develops and designs desktop and mobile platforms, which can help users obtain the diagnosis and treatment of minor health problems, and at the same time realize online consultation and obtain treatment prescriptions issued by doctors by paying a certain fee; An embedded biomedical sensor studied in Literature [15] realizes the acquisition of human physiological response and behavior data by carrying a patch and a smartphone, which can be applied in the fields of patient monitoring and clinical trials; [16] The combination of this sensor and APP can realize the management of chronic obstructive pulmonary disease and asthma and the tracking of patients' drug use, and can provide personalized health advice and optimize the treatment plan and treatment time according to the patient's condition.

Not only a physiological parameter of heart rate can be extracted from the pulse wave but also some other physiological parameters can be extracted. Literature [17] uses the camera to obtain the finger image information, and realizes the detection of human pulse, blood oxygen, and respiratory rate through pixel extraction of the image information and simulation of the photoplethysmographic wave signal. Literature [18] used the RGB three-primary color signal sequence on the skin surface to estimate the relative blood oxygen saturation with blue light as the Literature light. Literature [19] proposed a method to obtain blood pressure data by measuring PPG signal with a mobile phone. Because smartphones integrate a variety of sensors, in addition to using the camera and flashing lights of the mobile phone, we can also use the microphone of the mobile phone to measure the lung capacity of the human body. Literature [20] developed the software SpiroSmart, which collects the sound signal of deep breathing and uses machine learning regression to estimate the human vital capacity. With the rapid development of science and technology, researchers have applied some artificial intelligence methods originally used in condition monitoring and machine fault diagnosis to human disease diagnosis and monitoring. At present, these methods have achieved certain results in human health diagnosis and monitoring. Literature [21] proposed an adaptive hidden Markov model based on wearable multisensor devices and used it to prevent and manage chronic diseases. Literature [22] introduced the framework of Bayesian Hierarchical Poisson Models with Hidden Markov Structure to detect the onset of influenza flow.

3. Biometric Data Collection Model

In this study, the biometric data acquisition model is used to construct a health monitoring application, and the biometric data acquisition model is first analyzed.

Before constructing the associated motion association network, it is necessary to calculate the associated motion similarity network, that is, to calculate all the similarity matrices involving associated motions. For the calculation method of similarity between expression profiles, the linear transformation L learned from the association motion knockout and association motion overexpression data based on the LFDA algorithm is used to recalculate the similarity matrix between the association motion knockout expression profiles, and the correlation motion is obtained. In the experiments, we selected 3689 expression profiles of association motor knockout experiments in the MCF7 cell line and calculated the similarity magnitude of all association motor pairs.

Collected from the MSigDB database (version 5.1), all 5936 associated movements with GOBP annotation information constitute a set of GO BP, and 5039 associated movements with GO MF annotation information constitute a set of GPMF. We recorded the knockout on MCF7 in the LINCS data set. The 3689 associated motion sets of the experiment are LINCS, and the Venn diagram (1) represents the intersection of the three. We can analyze two of these subsets, one is the subset A of the associative motor knockout experiment in the LINCS data MCF7 cell line, and has GOBP or GOMF annotation information, and the other is the existing associative motor knockout experiment. There is also associated motion set subset B with GOBP annotation information. The number of elements in the two sets is 2304 and 1905, respectively, and the latter is a subset of the former.

According to the similarity network of the knockout expression profile of the association movement, we can cluster all the association movements according to the cluster analysis, and then construct the association movement association network according to the clustering results. Figure 1 shows the Venn diagrams involving associated motion sets in the three datasets.

According to the hypothesis, there should be similar annotation information of GOBP and GO MF. Therefore, we can perform cluster analysis on the associated motion set A and the associated motion set B, respectively. In the associated motion set A, there are 399 associated motions with unknown GOBP associated motion annotation information. It is the associated motion set whose GOBP annotation information can be predicted later. Moreover, we perform cluster analysis on the two sets, respectively, and we can use the two clustering results to verify the correctness of the clustering results in the subsequent analysis to verify the basic hypothesis.

We selected k-means clustering, spectral clustering, Non-Negative Matrix Factorization (NMF), and AP clustering for analysis. The k-means clustering algorithm and the spectral clustering algorithm cannot obtain stable clustering results during the experiment, so these two clustering methods are not suitable for the clustering analysis of the data. The NMF method is to first use the matrix non-negative decomposition to find the low-dimensional reconstruction of all associated motions, that is, to find the non-negative matrices w and H such that

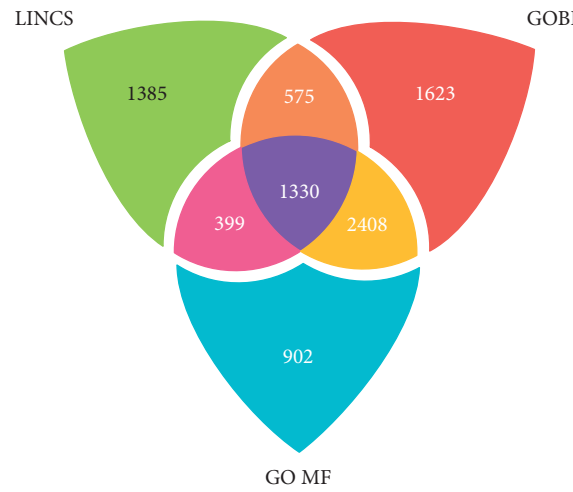

Figure 1: Venn diagrams involving associated motion sets in the three datasets.

$$V \approx WH, W \in R_{+}^{n\times k}, H \in R_{+}^{n\times k}. \quad (1)$$

Then, k-means clustering is performed with one of W/H as a low-dimensional representation of the associated motion. AP clustering is to find the best clustering result of each vertex through the data information propagation and product algorithm (sum-product algorithm) in the probabilistic graph model. The input to both algorithms is the similarity matrix of the samples. However, NMF and spectral clustering need to specify the number of clusters, while AP clustering will automatically choose the optimal number of clusters.

In the clustering process of the NMF method, we set the number of clusters to 9 k values with an interval of 10 from 20 to 100, performed 9 different NMFs, and obtained the performance investigation results of the method, as shown in Figure 2. In the performance survey graph, the larger the cophenetic coefficient, the better the decomposition effect. The RSS value needs to be as small as possible. Residuals represents the residual, which represents the deviation between the decomposed matrix and the original matrix, and also needs to be as small as possible. The consistency curve (Consensus) reflects its cluster consistency, which is a number between [0, 1]. The closer to 1, the better the consistency. Therefore, according to Figure 2, in terms of the number of clusters, the optimal number of clusters is around 80 to 90.

According to the above analysis, we can get the histogram of the coverage. From the Figure 3, we can see that there are 66 sub-communities whose coverage is higher than 0.8, and the remaining 18 sub-communities are lower than 0.8. That is, in the separate clustering analysis of the two sets, most of the clustering communities in the B set are covered by the corresponding large communities in the A set, and the two clustering results are consistent. The clustering results are valid, and the next step can be analyzed.

At the same time, we can compare the clustering performance of the similarity network based on the LFDA algorithm and the similarity network based on the ScoreGSEA algorithm. Figure 4 shows the consistency

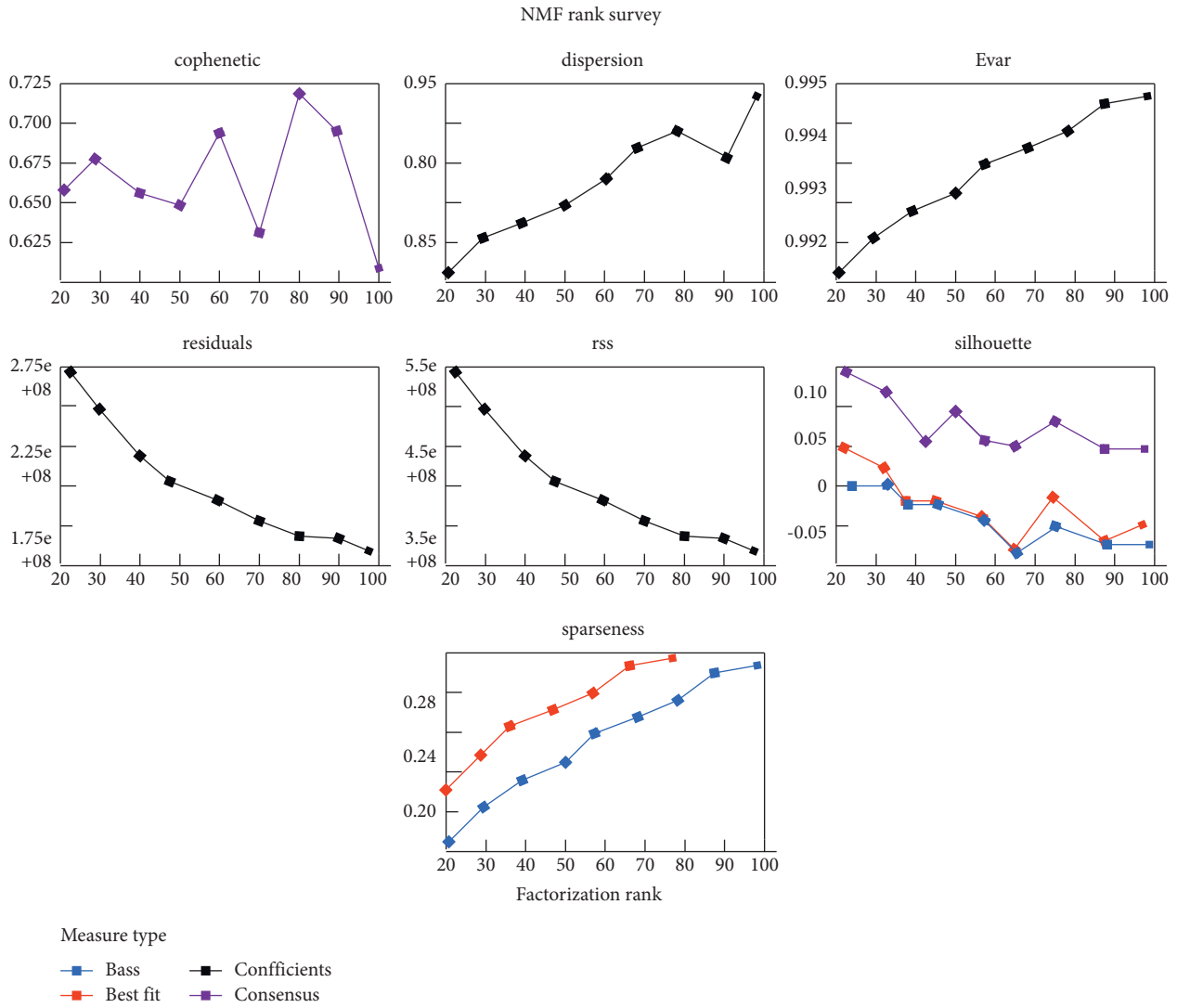

Figure 2: The NMF rank survey results show that the cophenetic coefficient peaks between 80 and 90, but the clustering consistency is consistently low. At the same time, when NMF decomposes the similarity matrix, no matter how many clusters are used, the consistency mainly fluctuates below 0.1, and the consistency of the clustering results is extremely poor, so the NMF method is not suitable for the study of this data.

results of the clustering results in the two sets based on the similarity network of the ScoreGSEA algorithm. Comparing the two figures, we can see that the consistency of the clustering results of the similarity network based on the LFDA method is significantly better than the corresponding results based on the ScoreGSEA algorithm.

After verifying the validity of the clustering, we also need to verify our basic assumptions. Figure 5 below shows the verification results.

Each community is the clustering result of cluster analysis, and two associated movements of the same community are represented by similarity, and they belong to the same class due to their high similarity. Therefore, according to the premise, the associated movement sets of the same community should have the same performance in Go terms, and the associated movements of different communities should have no intersection in GO Terms.

The above proves the validity of the clustering results and verifies the correctness of the basic assumptions. According to the clustering results of the cluster analysis, we can construct the association motion association network according to the communities obtained by clustering, as shown in Figure 6. Each vertex in the graph represents all the associated motions in the A set, each edge represents the similarity between vertices, and the vertices in each area constitute a community, and 10 major communities are drawn in the figure.

In the associative motion graph, the associated motions of each community's sub-communities (i.e., points in the B set) are represented by blue vertices, and these associated motions have known GOBP annotations. The rest of the vertices are represented by red vertices, and these associated motions are unknown for their GOBP annotation information. Through Enrichr's enrichment analysis, the

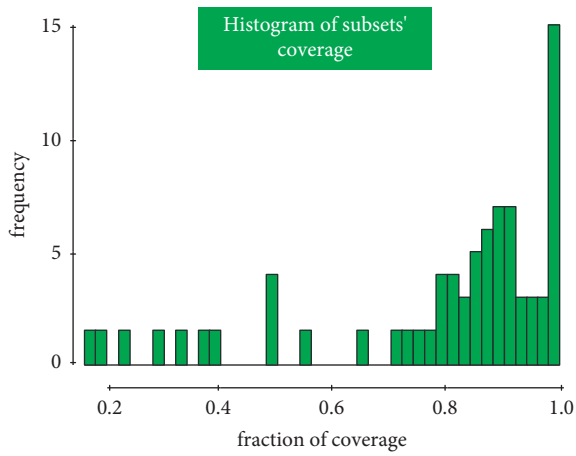

Figure 3: Histogram of coverage statistics of cluster communities in set B corresponding to cluster communities in set A.

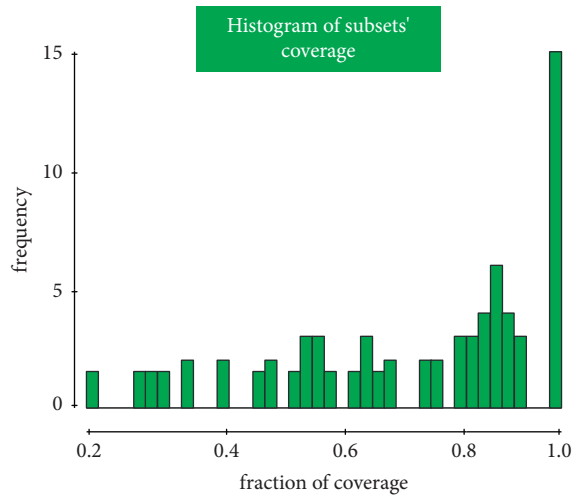

Figure 4: Histogram of coverage statistics of the clustering community in set B in the similarity network based on the ScoreGSEA algorithm in the corresponding clustering community in set A.

enrichment results of sub-communities with known GOBP information in the associated motion association network can be obtained. At the same time, it is speculated that the missing GOBP annotation information represented by the red vertices in the community is related to the GOBP annotation information of the movement. This is the GOBP annotation information prediction process of this model. Through the analysis of the clustering results, we verified the validity of the clustering results and the correctness of the basic assumptions, so the validity of this model has also been proved.

At the same time, we can also analyze the specificity of the clustering results. As shown in Figure 7, the abscissa represents the number of communities, and the ordinate represents the statistics of the number of GO Terms shared by several communities. It can be seen that nearly 500 GO Terms are exclusively within a single community, and the

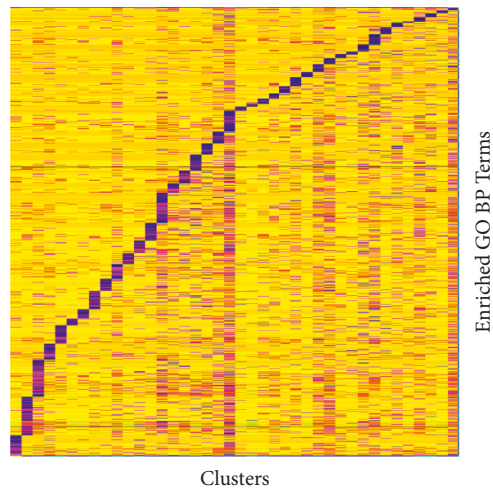

Figure 5: Heat map of the correlation between clustering results and GO BP enrichment results: the horizontal direction in the figure represents the clustering community, the vertical direction represents the term of GOBP, and the value in the heat map is the p value size of each community after enrichment analysis.

clustering results have high specificity and practical analysis significance.

Similar to generalized Mahalanobis distance, first we need to find a new feature space. In this space, the cosine value between samples satisfies that the cosine value between similar samples is high, and the cosine value between dissimilar samples is low. Therefore, we need to define a linear transformation $A \in R^{d\times n}$, that is, to map the original n-dimensional feature vector into a d-dimensional space:

$$A\colon R^n \longrightarrow R^d \,(d \le n). \tag{2}$$

Because $d \le n$, the transformation A also reduces the dimension of the feature data. At this point, the cosine values of samples x and y in the transform subspace are

$$CS(x, y, A) = \frac{(Ax)^T (Ay)}{\|Ax\| \cdot \|Ay\|} = \frac{x^T A^T Ay}{\sqrt{x^T A^T Ax}\sqrt{y^T A^T Ay}}. \tag{3}$$

The set of constraints is S, D. Our goal is to have high cosine values for similar samples and low cosine values for dissimilar samples. Then, there is an objective function:

$$f(A) = \sum_{(x,y)\in S} CS(x,y,A) - \alpha \sum_{(x,y)\notin D} CS(x,y,A) - \beta\|A - A_0\|. \tag{4}$$

Among them, $\alpha, \beta \ge 0$ is a hyperparameter, and $\|A - A_0\|$ is a regular term, which is used to control the distance between the target transformation A and the predefined matrix Ao, control the optimization step size, and prevent overfitting. The parameter α balances the contribution of the positive sample pair and the negative sample pair to the loss function. The optimal value can be determined by the cross-validation method, or it can be directly set to |SVD).

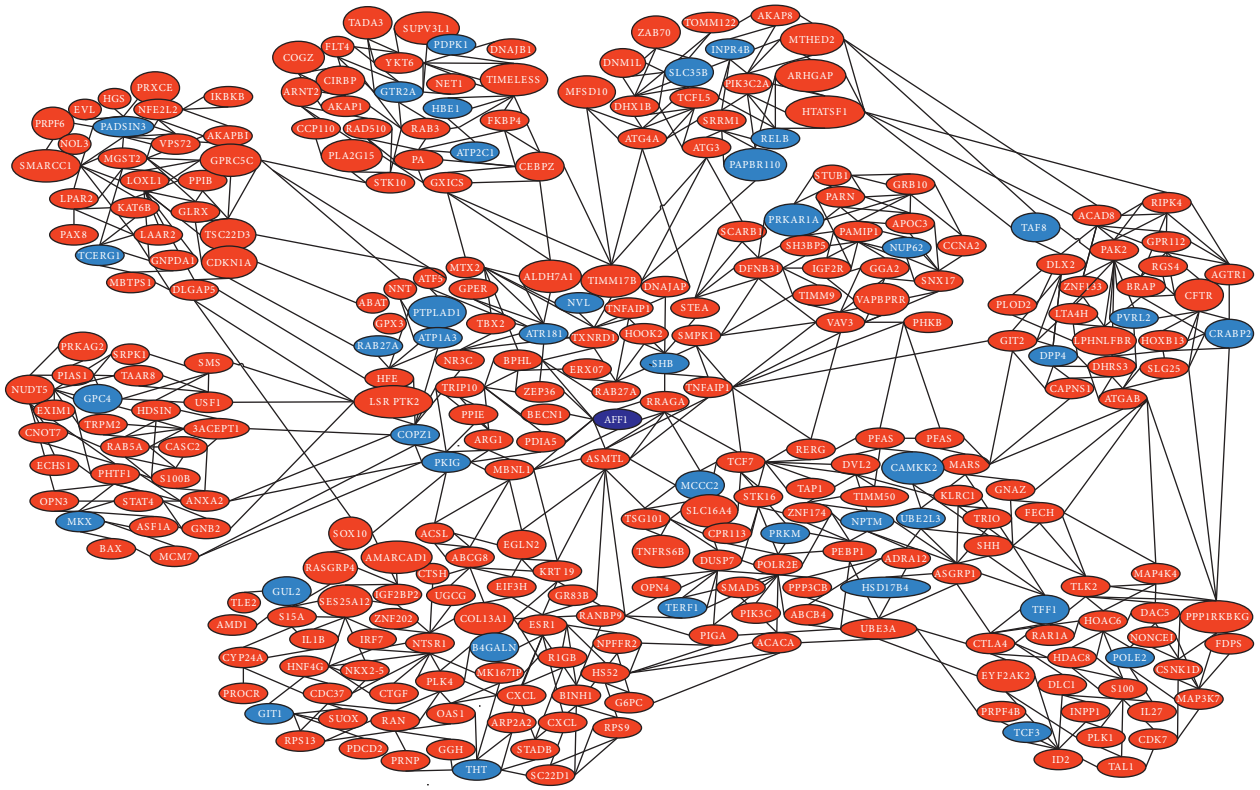

FIGURE 6: Display of the associated motion association network: because there are too many network vertices with 2304 associated motions, only 10 associations of the association network are shown in the figure, and the blue vertices are the associated motions of the known GO BPs.

Therefore, our final optimization goal is to find the transformation A^* that maximizes the objective function, namely:

$$A^* = \underset{A}{arg\,max}\ f(A). \tag{5}$$

Jaccard distance is used to define the similarity of ATC labels between motions:

$$J(d_i, d_j) = \frac{|l_i \cap l_j|}{|l_i \cup l_j|}. \tag{6}$$

Then, we can decide which set of constraints the two motions belong to according to the threshold 8, that is,

$$\begin{aligned} S &= \{(d_i, d_j) | J(d_i, d_j) > \delta\}, \\ D &= \{(d_i, d_j) | J(d_i, d_j) < \delta\}. \end{aligned} \tag{7}$$

We use ATC labels as side information to construct a restricted set, so the model is a weakly supervised algorithm.

The objective function (4) is divided into two parts: the loss function formed by the summation of cosine functions and the regular term. For a fixed predefined matrix Ao, the optimized optimal solution A^* performs better than A_0. Therefore, we use an iterative strategy to continuously optimize. That is, in the next iteration, the A^* value of the previous round is substituted into the new A_0 for calculation, and at the same time, cross-validation is used to ensure that the solution of each round is improving the performance. In addition, the coarse-to-fine strategy is used to update the β value during the iteration, and the β value finally approaches $+\infty$, so the iteration of A^* will eventually stabilize and obtain the final optimal solution.

The next step is to solve the optimal solution in step 4 in the Algorithm Table (1). First, we derive it with respect to the transformation matrix A, and obtain

$$\frac{\partial f(A)}{\partial A} = \sum_S \frac{\partial C\,S(x, y, A)}{\partial A} - \alpha \sum_D \frac{\partial C\,S(x, y, A)}{\partial A} - 2\beta(A - A_0). \tag{8}$$

Among them, the partial derivative with respect to A of a single cosine function is

$$\begin{aligned} \frac{\partial C\,S(x, y, A)}{\partial A} &= \frac{1}{v(A)} \frac{\partial u(A)}{\partial A} - \frac{u(A)}{v(A)^2} \frac{\partial v(A)}{\partial A} \\ &= A\left[\frac{1}{\|Ax\| \cdot \|Ay\|}\left(xy^T + yx^T\right)\right. \\ &\quad \left. - \frac{(Ax)^T Ay}{\|Ax\|^2 \|Ay\|^2}\left(\frac{\|Ay\|}{\|Ax\|} xx^T + \frac{\|Ax\|}{\|Ay\|} yy^T\right)\right]. \end{aligned} \tag{9}$$

The common factor in formula (9) is as follows:

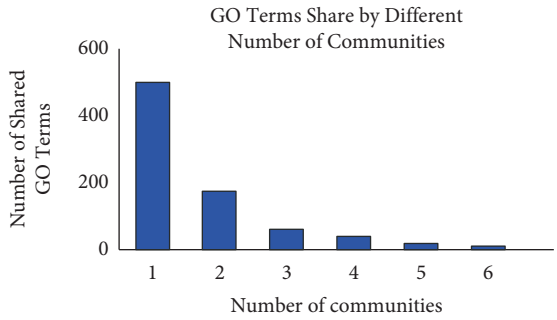

Figure 7: Statistical diagram on the frequency of community sharing of GO Terms.

$$M = \frac{1}{\|Ax\| \cdot \|Ay\|}\left(xy^T + yx^T\right) - \frac{(Ax)^T Ay}{\|Ax\|^2 \|Ay\|^2} \left(\frac{\|Ay\|}{\|Ax\|}xx^T + \frac{\|Ax\|}{\|Ay\|}yy^T\right). \tag{10}$$

From the analysis of formula (10), we can find that the norm and the inner product in the formula are both scalars, and the result of the vector product is a symmetric matrix. To sum up, we can do the following transformation on the derivative of the objective function:

$$\begin{cases} D = \sum_S M_i - \sum_D M_i - 2\beta E = d(A), \\ \beta = -2\beta A_0. \end{cases} \tag{11}$$

Among them, E is the identity matrix, then we can get the simplified formula of formula (8):

$$\frac{\partial f(A)}{\partial A} = AD - B. \tag{12}$$

Among them, $D = d(A)$ is a symmetric matrix, and it is a negative definite matrix when β is large enough. We want to find the extreme value of the objective function, that is, to find the point whose derivative is equal to zero, that is, to find the zero solution of the linear equation system (12). Because the negative definite matrix D is a function of the parameter matrix A, we use the iterative form of the Conjugate Gradient Method (ICGM) to solve the model, that is, to solve d linear equations:

$$DA^T(k) - B^T(k) = O, k = 1, 2, \ldots, d. \tag{13}$$

Among them, $A^T(k)$, $B^T(k)$ is the k-th column vector of matrix A^T, B^T, The solution process of ICGM is shown in Algorithm Table (2).

Algorithm (2) ensures that we can solve the stationary point of the objective function. However, by calculating the second derivative of its derivative, we can find that the objective function does not guarantee convexity, so the solution process of the problem can only obtain a local optimal solution. That is, the solution of the problem depends on the selection of the predefined matrix A_0.

The iterative conjugate gradient method is used to solve the linear equation system, and the direction of the optimized gradient in the original conjugate gradient method is orthogonal to the previous one each time. However, in the ICGM model, since the negative definite matrix D is related to the parameter matrix A, all of them are solved by an iterative method, but the orthogonality of each iteration direction is also lost. However, in fact, in the optimization process, the selection of the initial direction is based on the negative definite matrix D_j of the previous time, and in the calculation of the orthogonal direction in the next step, D_{j+1} is used as the coefficient matrix. Therefore, according to the characteristics of the conjugate gradient method, each optimization ensures that the residual error of the linear equation system is reduced, and finally a zero solution is reached. Figure 8(a) shows the change curve of the residual $R = D'A^T - B^T$ in the iterative process of the linear equation system in the optimization process, and the ordinate in Figure 8 is the logarithmic index. From Figure 8, we can see that despite the use of nonstrictly orthogonal search directions, the optimization speed is still very fast. In the matrix solution of rank 50, the allowable accuracy is achieved in only 32 iterations. At the same time, during the whole optimization process, the residual error is strictly reduced, which proves the correctness of this optimization method.

In the whole iterative process of the algorithm, each small iteration is the ICGM algorithm, and its first layer iterative method is the algorithm (1). The correctness of the algorithm is shown in Figure 8(b). After the optimal solution of the previous round of ICGM is substituted as a predefined matrix in a new round of iteration, its objective function rises steadily and meets the optimization objective, so it can be proved that the iterative strategy is effective.

4. Sports Personnel Health Monitoring Application Based on Biometric Data Collection Model

In this study, the construction of a sports personnel health monitoring application program is combined with the biometric data acquisition model. When designing the monitoring system, several principles were followed for the design, which mainly included the data acquisition part, the associated motion data transmission and the monitoring center part. The data acquisition part is mainly composed of the terminal node structure based on STM32 microprocessor, which includes LoRa wireless communication module and various sensor modules. The data transmission part is composed of an STM32-based associated motion microprocessor, which includes a LoRa wireless communication module and a WIFI module. The monitoring center is mainly constructed based on server-related motion, and corresponding monitoring functions can be realized by deploying a web server. The overall design structure of the system of this subject is shown in Figure 9(a).

The system software part includes the design of the terminal node data acquisition terminal, the aggregation node and the cloud server. The overall design block diagram of system software is shown in Figure 9(b).

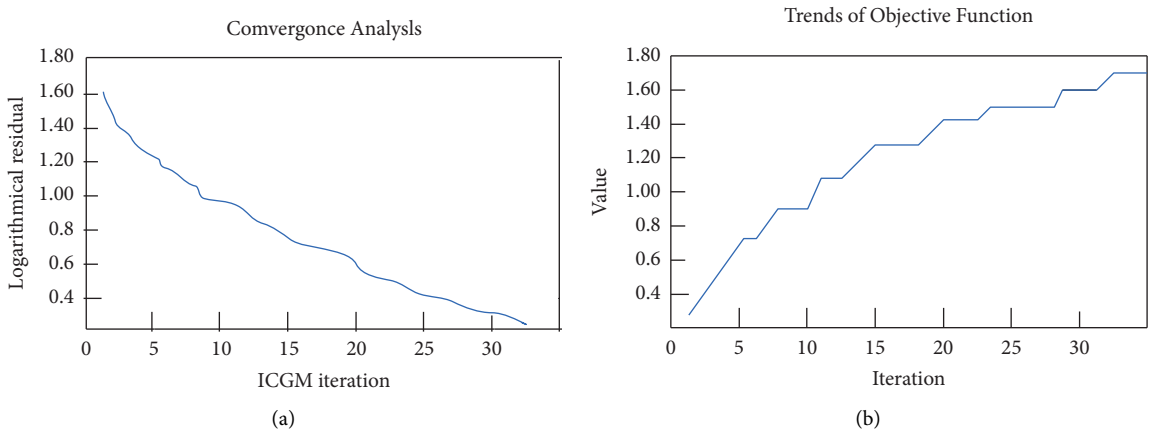

FIGURE 8: (a) In the optimization process of the iterative conjugate gradient method, the change trend of the residual R of the linear equation system, and the ordinate in the figure is the logarithmic index; (b) as the outer iteration proceeds, the overall objective function rises steadily.

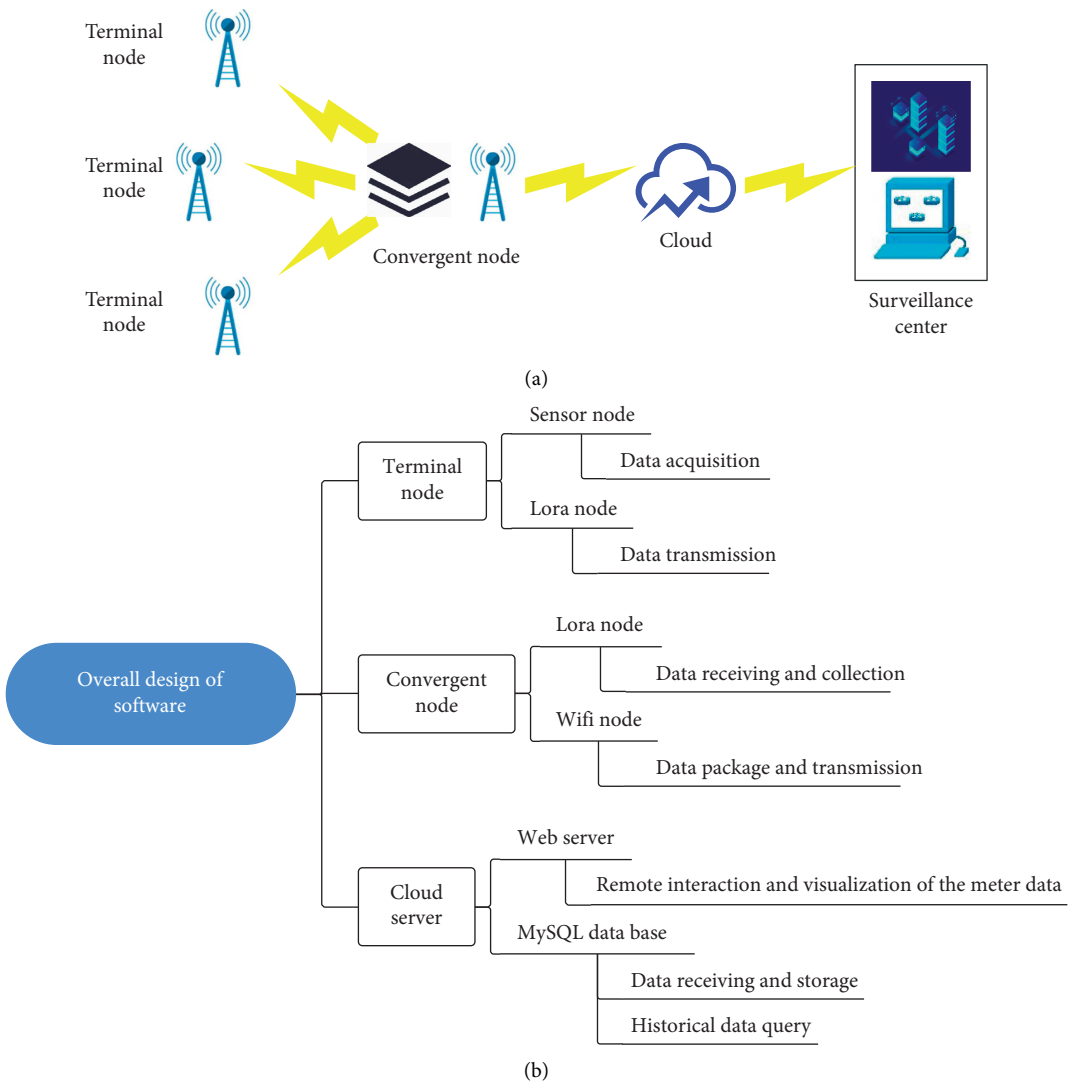

FIGURE 9: Structure of sports personnel health monitoring application program based on biometric data collection model. (a) System overall design architecture diagram and (b) system software design block diagram.

Table 1: The group sports data collection effect of the model.

Num	Data collection	Num	Data collection	Num	Data collection
1	87.95	20	90.00	39	87.74
2	84.37	21	84.36	40	88.92
3	91.46	22	88.34	41	86.79
4	86.85	23	84.11	42	88.36
5	84.49	24	86.24	43	89.44
6	87.50	25	85.17	44	84.27
7	90.42	26	89.43	45	90.47
8	88.86	27	86.88	46	91.84
9	87.56	28	89.49	47	90.28
10	91.91	29	86.59	48	91.74
11	87.20	30	85.96	49	85.35
12	90.00	31	84.62	50	88.91
13	91.23	32	85.50	51	84.77
14	89.16	33	86.06	52	86.01
15	85.47	34	90.73	53	85.34
16	90.73	35	91.23	54	84.88
17	84.21	36	85.84	55	90.34
18	84.46	37	86.77	56	85.72
19	87.96	38	88.66	57	84.07

Table 2: Health monitoring effect of sports personnel health monitoring application based on biometric data collection model.

Num	Motion monitoring	Num	Motion monitoring	Num	Motion monitoring
1	78.95	20	78.74	39	85.50
2	79.85	21	87.05	40	79.53
3	86.26	22	82.08	41	81.98
4	78.63	23	87.93	42	82.59
5	83.61	24	79.73	43	78.02
6	86.55	25	81.62	44	78.39
7	84.49	26	78.04	45	83.41
8	77.03	27	83.39	46	79.31
9	87.55	28	84.38	47	83.69
10	79.82	29	84.93	48	82.01
11	87.29	30	79.50	49	86.18
12	80.55	31	82.46	50	82.22
13	87.00	32	77.68	51	86.57
14	81.50	33	81.76	52	84.59
15	86.53	34	87.51	53	87.80
16	85.94	35	78.38	54	79.70
17	85.06	36	84.09	55	78.42
18	81.32	37	79.61	56	83.85
19	86.39	38	84.40	57	80.26

After constructing the above model, this study verifies the collection effect of group sports data of the biometric data collection model proposed in this study, and calculates the data collection evaluation results as shown in Table 1.

The above verifies that the sports personnel health monitoring application based on the biometric data collection model has a good effect of group sports data collection. On this basis, this study verifies the health monitoring effect of the sports personnel health monitoring application based on the biometric data collection model, and obtains the results shown in Table 2.

From the above research, it can be seen that the sports personnel health monitoring application based on the biometric data collection model proposed in this study has a good health monitoring effect, and has an important supporting role in improving the fitness effect of group sports.

5. Conclusion

The application of the Internet of Things technology in the sports and fitness industry focuses on the main body with the attribute of "thing" in the fitness system. It is based on the gradually mature information system, and it is supplemented by the application of the core technology of the Internet of Things, and follows the principle of demand orientation, and finally realizes "smart sports." The body area network is "a wireless network based on a wireless sensor network, a wireless network formed by sensors for collecting physiological parameters on the human body or

biosensors transplanted into the human body," which can be used as an information communication solution for a ubiquitous physical health monitoring system. This study combines the biometric data acquisition model to construct the sports personnel health monitoring application program to improve the sports personnel health monitoring effect. The research shows that the sports personnel health monitoring application based on the biometric data collection model proposed in this study has a good health monitoring effect, and has an important supporting role in improving the fitness effect of group sports.

Data Availability

The experimental data used to support the findings of this study are available from the corresponding author upon request.

Conflicts of Interest

The author declared that there are no conflicts of interest regarding this work.

References

[1] D. Henriques-Neto, J. P. Magalhães, M. Hetherington-Rauth, D. A. Santos, F. Baptista, and L. B. Sardinha, "Physical fitness and bone health in young athletes and nonathletes," *Sport Health*, vol. 12, no. 5, pp. 441–448, 2020.

[2] T. M. Kravchuk, N. M. Sanzharova, J. V. Golenkova, and I. B. Katrechko, "Influence of means of parterre gymnastics on physical fitness of young athletes in acrobatic rock and roll," *Health, sport, rehabilitation*, vol. 6, no. 3, pp. 19–25, 2020.

[3] D. Okun and K. Mulyk, "Investigation of the relationship between the indicators of physical preparedness and the basic technique elements of young water-slalom athletes," *Slobozhanskyi Herald of Science and Sport*, vol. 5, no. 61, pp. 69–71, 2017.

[4] O. Politko, "Model characteristics of physical development and special physical preparedness of swimmers 12–15 years old," *Slobozhanskyi Herald of Science and Sport*, vol. 2, no. 64, pp. 37–40, 2018.

[5] G. Chang, "Retracted article: urban air pollution diffusion status and sports training physical fitness measurement based on the Internet of things system," *Arabian Journal of Geosciences*, vol. 14, no. 16, pp. 1555–1611, 2021.

[6] B. Silva and F. M. Clemente, "Physical performance characteristics between male and female youth surfing athletes," *The Journal of Sports Medicine and Physical Fitness*, vol. 59, no. 2, pp. 171–178, 2019.

[7] L. P. Tuti Ariani, "The effect of repetition sprint training method combined with the level of physical fitness toward the speed of 100 meter run," *International Journal of Engineering, Science and Information Technology*, vol. 1, no. 3, pp. 59–63, 2021.

[8] Z. L. Kozina, M. Cieslicka, K. Prusik et al., "Algorithm of athletes' fitness structure individual features' determination with the help of multidimensional analysis (on example of basketball)," *Physical education of students*, vol. 21, no. 5, pp. 225–238, 2017.

[9] A. V. Titova, O. G. Chorniy, A. A. Dolgov et al., "Parameters of biochemical control as a criteria of adaptive changes in the organism of athletes with various fitness levels engaged in the conditions of power fitness," *Ukraïns'kij žurnal medicini, biologiï ta sportu*, vol. 3, no. 2, pp. 278–283, 2018.

[10] T. Chernykh, V. Mulik, and D. Okun, "Study of the level of physical fitness of young acrobat athletes at the initial stage of training," *Slobozhanskyi Herald of Science and Sport*, vol. 7, no. 73, pp. 27–30, 2019.

[11] P. Kostiantyn, G. Grygoriy, P. Vasyl et al., "Correlation analysis of readiness indicators of athletes and their competitive results in kettlebell sport," *Journal of Physical Education and Sport*, vol. 17, no. 3, pp. 2123–2128, 2017.

[12] L. A. Sarafyniuk, A. V. Syvak, Y. I. Yakusheva, and T. I. Borejko, "Correlations of cardiointervalographic indicators with constitutional characteristics in athletes of mesomorphic somatotype," *Biomedical and biosocial anthropology*, no. 35, pp. 17–22, 2019.

[13] V. V. Artiuh, Z. L. Kozina, V. O. Koval, D. V. Safronov, S. V. Fomin, and Y. O. Novikov, "Influence of application of special means of development of equilibrium and precision-target movements on the level and structure of psychophysiological indicators, physical and technical readiness of archers," *Health, sport, rehabilitation*, vol. 4, no. 4, pp. 7–16, 2019.

[14] Y. Strykalenko, O. Shalar, V. Huzar, R. Andrieieva, I. Zhosan, and S. Bazylyev, "Influence of the maximum force indicators on the efficiency of passing the distance in academic rowing," *Journal of Physical Education and Sport*, vol. 19, no. 3, pp. 1507–1512, 2019.

[15] F. Fachrezzy, I. Hermawan, U. Maslikah, H. Nugroho, and E. Sudarmanto, "Profile physical fitness athlete of slalom number water ski," *International Journal of Educational Research & Social Sciences*, vol. 2, no. 1, pp. 34–40, 2021.

[16] R. L. Kons, E. Franchini, and D. Detanico, "Relationship between physical fitness, attacks and effectiveness in short- and long-duration judo matches," *International Journal of Performance Analysis in Sport*, vol. 18, no. 6, pp. 1024–1036, 2018.

[17] Z. Kozina, I. Sobko, L. Ulaeva et al., "The impact of fitness aerobics on the special performance and recovery processes of boys and girls 16-17 years old engaged in volleyball," *International Journal of Applied Exercise Physiology*, vol. 8, no. 1, pp. 98–113, 2019.

[18] V. I. I. Zalyapin, A. P. Isaev, A. S. Bakhareva, and A. S. Aminova, "Modelling the spectral characteristics of the circulatory system of athletes-skiers," *Journal of Computational and Engineering Mathematics*, vol. 6, no. 4, pp. 57–68, 2019.

[19] P. Kyzim and S. Humeniuk, "Characteristics of the leading factors of special physical preparedness of athletes from acrobatic rock and roll at the stage of preliminary basic training," *Slobozhanskyi Herald of Science and Sport*, vol. 7, no. 71, pp. 20–24, 2019.

[20] D. Detanico, R. L. Kons, D. H. Fukuda, and A. S. Teixeira, "Physical performance in young judo athletes: influence of somatic maturation, growth, and training experience," *Research Quarterly for Exercise & Sport*, vol. 91, no. 3, pp. 425–432, 2020.

[21] E. A. Bondareva, O. I. Parfenteva, A. V. Kozlov et al., "The Ala/Val polymorphism of the UCP2 gene is reciprocally associated with aerobic and anaerobic performance in athletes," *Human Physiology*, vol. 44, no. 6, pp. 673–678, 2018.

[22] R. L. Kons, D. Detanico, J. Ache-Dias, and J. Dal Pupo, "Relationship between physical fitness and match-derived performance in judo athletes according to weight category," *Sport Sciences for Health*, vol. 15, no. 2, pp. 361–368, 2019.